

## Surface electronic structure of Ce in the $\alpha$ and $\gamma$ phase

Olle Eriksson, R. C. Albers, and A. M. Boring

*Center for Materials Science and Theoretical Division, Los Alamos National Laboratory, Los Alamos, New Mexico 87545*

G. W. Fernando

*Brookhaven National Laboratory, Upton, New York 11973*

Y. G. Hao and B. R. Cooper

*Department of Physics, West Virginia University, Morgantown, West Virginia 26506*

(Received 16 July 1990)

The surface electronic structure of Ce in the  $\alpha$  and  $\gamma$  phase has been calculated using a film linearized-muffin-tin-orbitals method. The bonding in Ce is found to be mainly metallic in character. The width of the  $4f$  band in  $\alpha$ -Ce is found to be about 0.7 eV both in the bulk and at the surface; in  $\gamma$ -Ce it is slightly narrower, about 0.6 eV. The calculated work function of  $\alpha$ -Ce is in good agreement with experimental data. Cross sections for the bremsstrahlung isocromat (BIS) processes have been calculated in a fully relativistic framework, and good agreement with experiment is obtained for the itinerant peak in the BIS data near  $E_F$ . We find our results consistent with an itinerant  $f$ -electron picture for  $\alpha$ -Ce, and thereby consistent with a picture for the  $\gamma \rightarrow \alpha$  transition that is from localized (and magnetic) to itinerant (bonding and nonmagnetic)  $f$ -electron behavior, i.e., a Mott transition, as opposed to a Kondo volume collapse picture involving a transition between localized states of the  $f$  electrons. We also predict that the surface of  $\alpha$ -cerium is  $\gamma$ -like.

### I. INTRODUCTION

Cerium, which is the first element in the lanthanide series with a  $4f$  electron, has a very complex phase diagram.<sup>1</sup> Depending on pressure and temperature it can be either an antiferromagnet, a temperature-independent paramagnet, or a superconductor. Furthermore, Ce is the only pure element to exhibit a solid-solid critical point. At atmospheric pressure and low temperatures the  $\alpha$  phase (fcc structure) is stable, and it behaves as an enhanced Pauli paramagnet. With increasing temperature  $\alpha$ -Ce transforms to the  $\beta$  phase (dhcp), and then to the  $\gamma$  phase (fcc). The  $\beta$  and  $\gamma$  phases show magnetic behavior; their susceptibilities follow a Curie-Weiss law with an effective Bohr magneton number close to the free-ion value, which indicates that the  $4f$  electrons are localized. At room temperature and a pressure of 7 kbar the trivalent low-density  $\gamma$  phase collapses into the much denser isostructural  $\alpha$  phase, with a volume decrease of about 14%. A further increase of pressure transforms<sup>2</sup>  $\alpha$ -Ce to  $\alpha'$ -Ce (orthorhombic) at 56 kbar or<sup>3</sup> to  $\alpha''$ -Ce (body centered monoclinic) at 50 kbar. The  $\alpha'$  phase has been shown<sup>4</sup> to exhibit superconductivity below 1.9 K.

Much of the theoretical work on this material has been focused on the unusual isostructural  $\gamma$ - $\alpha$  transition. In this transition, not only are the volumes very different for the two phases, but the magnetic and transport properties change as well. For instance, as stated above, the susceptibility of  $\gamma$ -Ce obeys a Curie-Weiss law, whereas  $\alpha$ -Ce is a temperature-independent paramagnet. Furthermore, the electronic specific-heat coefficient is 12.8 mJ/g at. K<sup>2</sup> for  $\alpha$ -Ce, which is larger than the value of 7.5 mJ/g at. K<sup>2</sup> obtained for  $\gamma$ -Ce. These dramatic changes in

physical properties were initially suggested<sup>5</sup> to be caused by the promotion of a localized  $4f$  electron in  $\gamma$ -Ce [ $4f^1(sd)^3$ ] to the conduction band in  $\alpha$ -Ce [ $4f^0(sd)^4$ ]. The loss of a localized  $4f$  electron together with an increase in the number of bonding valence electrons was thought to explain both the magnetic and bonding properties (the volume collapse). However, it was later pointed out that any type of promotional model for the  $\gamma$ - $\alpha$  transition is in serious conflict with the measured cohesive properties.<sup>6</sup> Also, experiments probing the electron density have since shown that the number of  $4f$  electrons remains practically unchanged during the transition and hence rule out the promotional model.<sup>7</sup> Therefore, it was suggested that the  $\gamma$ - $\alpha$  transition in Ce might be a Mott transition with the  $4f$  electrons being localized (nonbonding) in  $\gamma$ -Ce and itinerant (bonding) in  $\alpha$ -Ce.<sup>6,7</sup> Among other things, this suggests that the electronic structure of  $\alpha$ -Ce can be well described using a one-electron band picture. Indeed, this is what Glötzel<sup>8</sup> found, since his self-consistent relativistic calculation of  $\alpha$ -Ce gave a theoretical volume in good agreement with experimental data. Also, it was found that the  $4f$  band spin polarizes at the  $\gamma$ -Ce volume, which gives a Van der Waals loop in the calculated equation of state. However, a Maxwell equal area construction gave a volume collapse far too small and a transition pressure too low compared to the experimental data. Subsequent band calculations on Ce showed essentially the same results.<sup>9</sup> By implementing the orbital-polarization formalism<sup>10</sup> into a fully relativistic, spin-polarized band scheme, a good account of the  $\gamma$ - $\alpha$  transition was obtained.<sup>11</sup> Hence, these self-consistent, parameter-free calculations supported the Mott transition model and offered an alternative explana-

tion to the Kondo volume-collapse picture.<sup>12</sup>

Ce alloys and compounds have very many different ground states and complex phase diagrams.<sup>13</sup> This demonstrates the sensitivity of the physical and chemical properties of Ce materials to the environment, such as crystal structure, pressure, temperature, and chemical surrounding. For this reason we expect that the surface electronic structure of pure Ce should be equally complicated and interesting; the low coordination of the surface atoms should have an important effect on the electronic structure. In anticipation of further study including spin and orbital polarization effects, here we investigate the theoretically expected surface electronic structure of  $\alpha$  and  $\gamma$  cerium in the absence of such polarization effects. In part, this work is directed toward determining whether the experimentally observed work function for  $\alpha$  cerium is consistent with the  $f$  electrons having band (itinerant) behavior. As far as we know this paper is the first to explore the theoretically expected surface electronic structure of cerium in detail within a one-electron approximation. Because it is the first we have focussed here on the rudimentary aspects of the electronic structure. It is well known that Ce is very reactive and will tend to easily oxidize its surface, making surface work particularly difficult. Probably for this reason, it is also not known whether the surface reconstructs or whether the outermost layers expand outward. In this paper we also ignore these questions and treat the surface in an idealized manner, truncating the bulk structure to form the surface and placing the surface layer atoms in the same positions they would have in the absence of the surface. An interesting question raised by the present work is whether the surface of  $\alpha$ -Ce will undergo a transition to a magnetically polarized  $\gamma$ -like state. We intend to pursue this question in a spin and orbitally polarized total energy study for which the present work provides both necessary preparation and motivation.

## II. DETAILS OF THE CALCULATIONS

In this paper we report calculations on the surface electronic structure of Ce at two volumes, corresponding to that of  $\alpha$ - and  $\gamma$ -Ce. The electronic structure was calculated using the film linearized muffin-tin orbitals method<sup>14</sup> on a five-layer slab with a (100) orientation of an fcc crystal. With 16 muffin-tin orbits per atom and 14 plane waves, the calculation employed 94 basis functions. Since the calculation incorporated spin-orbit coupling we had to diagonalize  $188 \times 188$  matrices. The warped potential was calculated according to Ref. 14, within the local-density approximation and with the parametrization of Vosko-Wilk-Nusair.<sup>15</sup> In these relativistic (including the spin-orbit coupling), self-consistent calculations, the irreducible part of the two-dimensional Brillouin Zone was sampled at 10 special  $k$  points. The core electrons were furthermore recalculated at each iteration, by solving the radial Dirac equation. The cross section for the BIS process was calculated from the self-consistent potentials, in the same way as described in Ref. 16 (in a relativistic framework). The partial state densities of state (DOS) were multiplied with these cross sec-

tions and finally broadened (see below) to simulate the spectrometer resolution.

## III. RESULTS

We first turn our attention to the basic electronic structure. In Figs. 1 and 2 the calculated density of states (DOS) for  $\alpha$ - and  $\gamma$ -Ce are shown, respectively. For both systems the spin-orbit splitting of the  $4f$  orbitals is appreciable ( $\sim 0.4$  eV) when compared to the  $4f$  bandwidth, which indicates that relativistic effects are important and is why we included them. Furthermore, we find that the  $4f$  bandwidth (defined as the full width at half maximum of the  $4f$  projected DOS) of bulk  $\alpha$ -Ce is about 0.7 eV; the bandwidth of bulk  $\gamma$ -Ce is slightly narrower ( $\sim 0.6$  eV). These findings are in agreement with earlier calcula-

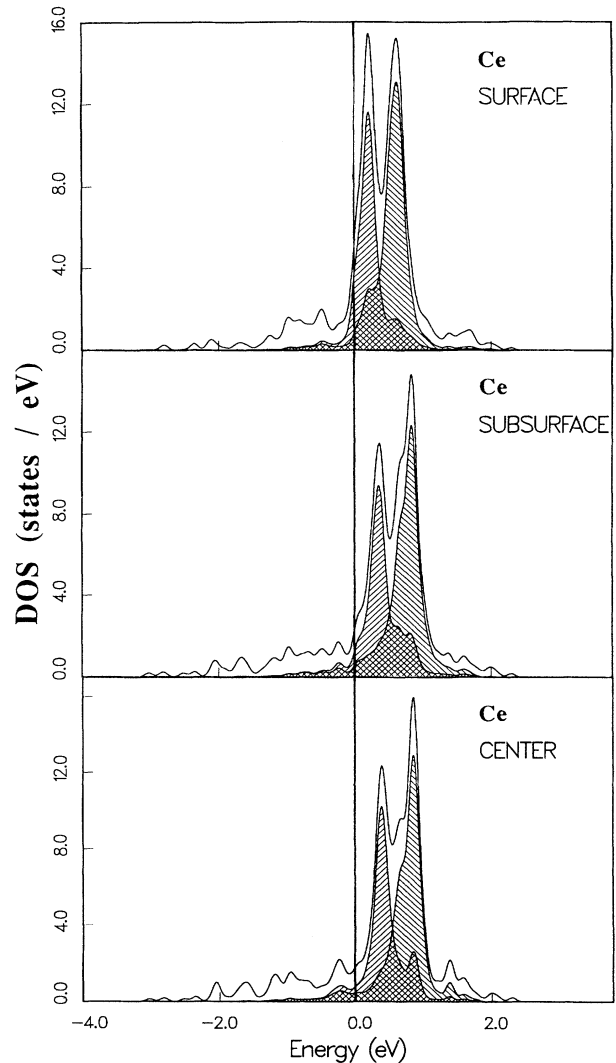


FIG. 1. Calculated DOS of  $\alpha$ -Ce. The bulk, subsurface, and surface DOS are shown in the bottom to top panels, respectively. The  $4f_{5/2}$  partial DOS is hatched from left to right whereas the  $4f_{7/2}$  DOS is hatched from right to left. Energies are in electron volts and  $E_F$  is at zero.

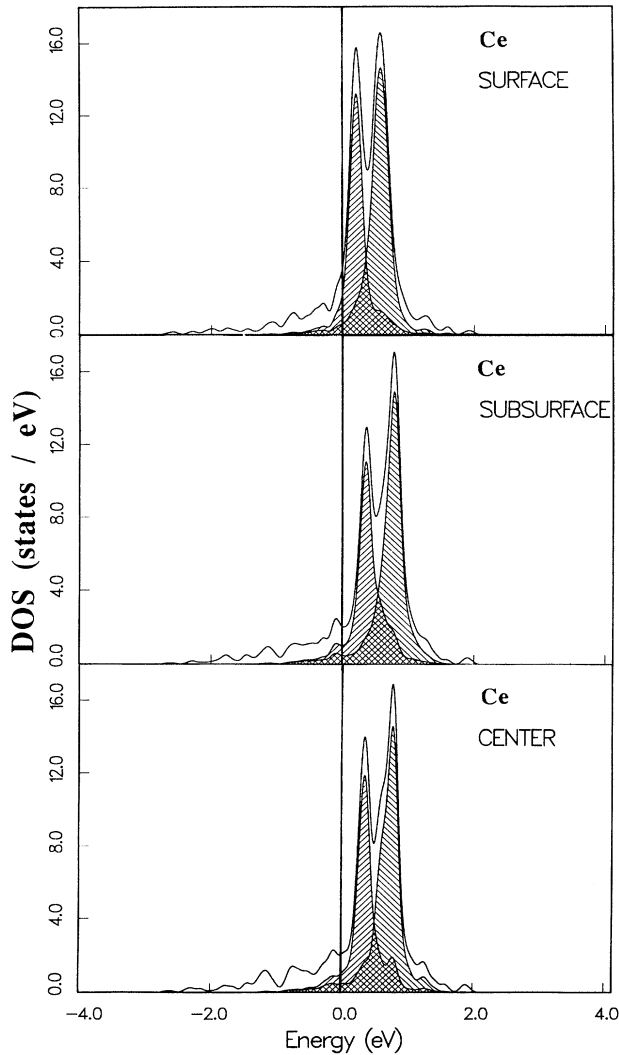


FIG. 2. Calculated DOS of  $\gamma$ -Ce. The bulk, subsurface, and surface DOS are shown in the bottom to top panels, respectively. The  $4f_{5/2}$  partial DOS is hatched from left to right whereas the  $4f_{7/2}$  DOS is hatched from right to left. Energies are in electron volts and  $E_F$  is at zero.

tions<sup>8,9</sup> that explored the electronic structure of bulk Ce. Since we do not allow spin polarization or any other degrees of freedom in our calculations, we expect that calculations for the two phases will only differ quantitatively and not qualitatively; band structures are usually a continuous function of parameters such as cell volume; which is the only way we have to distinguish the two phases in our calculations. As can be seen in Table I, the expansion of the fcc lattice on going to  $\gamma$ -cerium is accompanied by a substantial increase in the interstitial charge.

The main surprise in our calculations is that the surface projected DOS for  $\alpha$ - and  $\gamma$ -Ce have a  $4f$  bandwidth similar to that of their respective bulk values. This is in contrast to what we have found previously in other  $f$ -electron systems, viz., Pu and U, where a more pro-

TABLE I. Occupation numbers for  $\alpha$ - and  $\gamma$ -Ce. The interstitial charge is for 5 atoms per cell.

		$n_s$	$n_p$	$n_d$	$n_f$
$\alpha$ -Ce	Bulk	0.36	0.16	1.60	1.03
	Subsurface	0.35	0.16	1.46	1.04
	Surface	0.23	0.10	1.58	1.12
	Interstitial		4.53		
	Vacuum		0.24		
$\gamma$ -Ce	Bulk	0.24	0.13	1.31	0.90
	Subsurface	0.29	0.13	1.15	0.93
	Surface	0.21	0.10	1.24	1.04
	Interstitial		6.82		
	Vacuum		0.42		

nounced narrowing of the surface states was found.<sup>17</sup> As discussed below, this difference in behavior can be understood on the basis that the spin-orbit splitting is quite important for determining the overall  $4f$  bandwidth.

If we examine  $4f$  occupations, we find, as shown in Table I, that Ce has approximately one  $4f$  electron inside each muffin-tin radius. These  $4f$  occupation numbers are usually determined by the strong Hartree Coulomb energies of the  $4f$  orbitals and consequently are often relatively insensitive to geometrical effects such as crystal phase structure. In the bulk this  $4f$  electron count comes from states which have energies lower than the main  $4f$  peak shown in Figs. 1 and 2. The  $4f$  states at these lower energies are caused by hybridization with the conduction band ( $6s$  and  $5d$  orbitals) and are sometimes referred to as the "hybridization tail" of the  $4f$  band. However, it is clear from Figs. 1 and 2 that this  $4f$ -( $6s5d$ ) hybridization tail is weaker for the Ce surface atoms relative to that for bulk atoms for both phases. Therefore, in order to fill the approximately one  $4f$  electron in the surface states that are required by Coulomb energy considerations, the Fermi level ( $E_F$ ) will need to cut the surface projected DOS at the steep upturn of the  $4f_{5/2}$  partial DOS. Effectively, this means that the main peak of the  $4f$  band moves to lower energies at the surface in order to move down onto the Fermi energy. This causes the value of the DOS at  $E_F$  to increase for the surface states, which in turn, from a simpler Stoner theory, would predict that the surface atoms of  $\alpha$ -Ce should become spin polarized, in the same way that Glötzel found for bulk  $\gamma$ -Ce.<sup>8</sup> We would also make a similar prediction for the surface of  $\gamma$ -Ce except that the bulk is already normally presumed to be localized and this surface effect just more strongly enhances this same tendency. The basic surface electronic structure of the two phases revealed by Figs. 1 and 2 is otherwise very similar. Even the value of the DOS at  $E_F$  is about the same (about 4.0 states/eV).

In an attempt to elucidate the cause of the  $4f$  bandwidth we have made some additional calculations. In Fig. 3 we show three densities of states. Although all three were generated from the same fully relativistic self-consistent starting potential, they were calculated using different electronic structure approximations in a single iteration (i.e., they were not iterated to self consistency from the starting potential). Figure 3(a) (case a: the fully

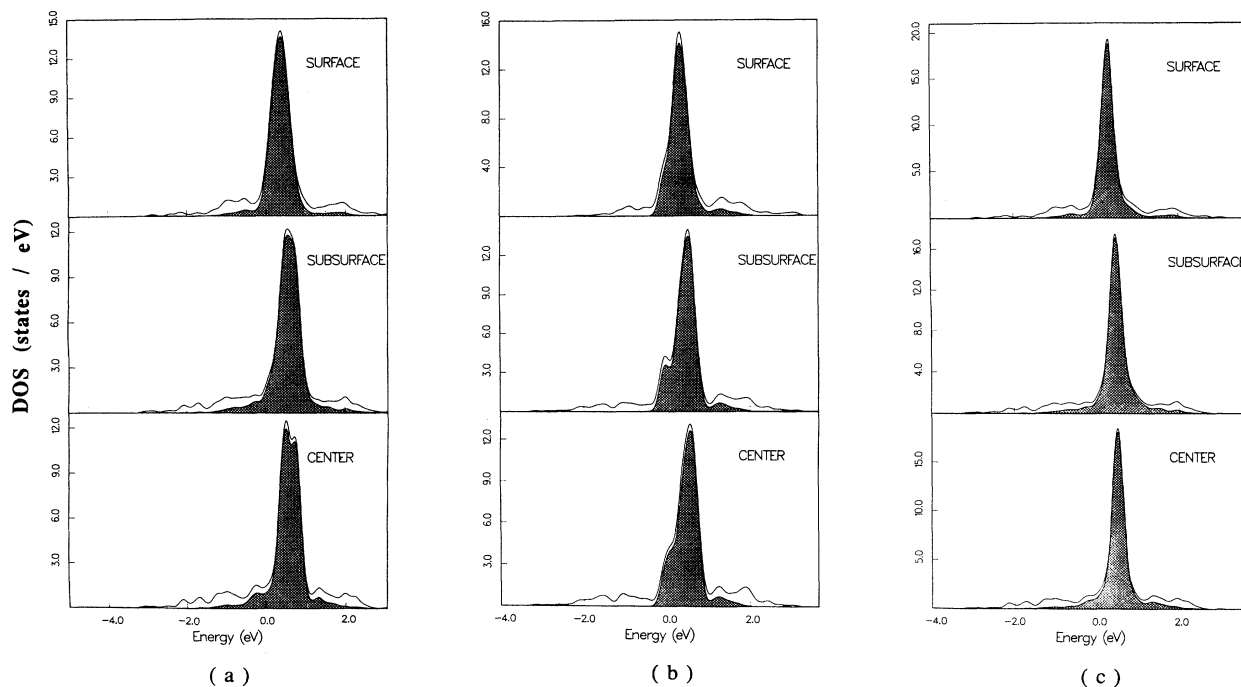


FIG. 3. (a) Calculated DOS of  $\alpha$ -Ce from a scalar relativistic calculation, (b) a scalar relativistic calculation with the hybridization between the  $4f$  states and all other states removed, and (c) a scalar relativistic calculation with the  $4f$  structure constants set to zero. The bulk, subsurface, and surface DOS are shown in the bottom to top panels, respectively. Energies are in electron volts and  $E_F$  is at zero.

hybridized case) was generated from a normal scalar-relativistic calculation, Fig. 3(b) (case b: the unhybridized  $f$ -band case) from a scalar-relativistic calculation where the hybridization of the  $4f$  states with all other orbitals was forced to be zero, and Fig. 3(c) (case c: the no  $4f$ - $4f$  hopping case) from a scalar-relativistic calculation with the  $4f$  structure constants set to zero. Comparing these three results allows us to isolate some of the different mechanisms that contribute to the formation of the  $4f$  band. For instance, we notice in Fig. 3 that the unhybridized bandwidth (case b) is about 15% narrower than the fully hybridized bandwidth (case a), and the bandwidth of the calculation with no  $4f$ - $4f$  hopping (case c) is about 70% of the fully hybridized calculation (case a). Notice also that the surface projected DOS of the fully hybridized scalar-relativistic calculation is narrower than the bulk projected DOS (0.53 eV for the surface DOS and 0.59 eV for the bulk). This effect is more pronounced in the scalar-relativistic case [Fig. 3(a)] than in the fully relativistic case (Fig. 1). The reason for this is that the bandwidth for the fully relativistic case is strongly affected by the spin-orbit splitting, which splits the  $4f$  band into its  $4f_{5/2}$  and  $4f_{7/2}$  components (Figs. 1 and 2) and the single  $4f$  DOS peak separates into two overlapping but clearly distinguishable subbands. In the scalar relativistic case this effect is absent and the  $4f$  DOS is characterized by just the one single peak (Fig. 3). The spin-orbit splitting also makes the bandwidths in Fig. 1 broader than in Fig. 3.

Turning to considerations of the chemical bonding we

note in Fig. 4 that the charge density for both  $\alpha$ - and  $\gamma$ -Ce is almost spherically symmetric with very little covalent or directional character. This is characteristic of metallic bonding. We also notice that a very sensitive probe of the charge density would indicate that the surface of both  $\alpha$ - and  $\gamma$ -Ce is more or less flat. This is a reflection of the large screening effects associated with metallic systems (covalent systems such as Si show a different behavior of the charge density, with “dangling bonds” sticking out into the vacuum).

We have calculated work functions for the two phases of Ce and find 3.5 eV for  $\alpha$ -Ce and 4.2 eV for  $\gamma$ -Ce. The  $\alpha$ -Ce value can be considered to be in satisfactory agreement with the experimental value of 3 eV, measured from a polycrystalline sample.<sup>18</sup> Ideally, the comparison should be made for a single crystal with the same orientation as in the calculation but to our knowledge no such measurements have been made for Ce. Comparing to the polycrystalline value is therefore somewhat uncertain, since crystallites with different orientation might show some anisotropy in the work function. As a matter of fact, our calculated work functions for (100) and (111) surfaces of Pu show anisotropy,<sup>17</sup> with work functions of 3.7 and 4.1 eV, respectively. One should also be aware of difficulties in comparing the experimental and theoretical work functions caused by possible experimental uncertainties in oxide and other surface contaminations for such a reactive material as Ce as well as because no reconstruction or relaxation of the surface atoms has been taken into account theoretically.

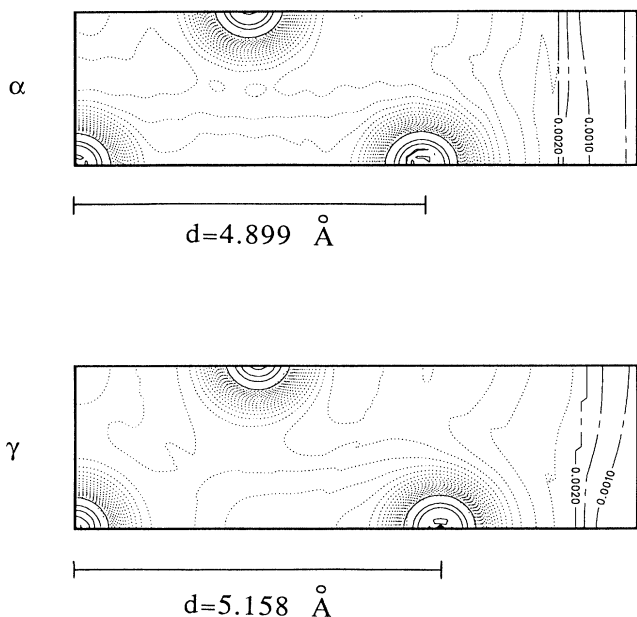


FIG. 4. Charge density [in electron/(a.u.)<sup>3</sup>] contour map for  $\alpha$ - and  $\gamma$ -Ce, cut along the (100) direction. The surface is to the right in the figure. The spacing between solid lines is 0.07, between dotted lines 0.003, and between broken lines 0.0005 (a.u.)<sup>3</sup>.

The difference in the calculated work functions between  $\alpha$ - and  $\gamma$ -Ce is quite substantial ( $\sim 0.7$  eV). This difference reflects the fact that the  $4f$  band is pushed up in energy when the volume decreases, and therefore  $E_F$  will also move up in energy. The difference between the potential at infinity and  $E_F$  decreases correspondingly, and  $\alpha$ -Ce has a lower work function. The increased amount of vacuum charge for  $\gamma$ -Ce is also consistent with an increased work function, since thereby the surface dipole moment increases and therefore also the work function. The good agreement between the calculated and measured work function is a useful check on our results, since this property is a very sensitive test of the quality of the calculation. Hence, the reasonably good agreement is consistent with the appropriateness of a  $4f$  band picture for  $\alpha$ -Ce. Additional corroboration is provided by the results of calculations on  $\alpha$ -Ce with the  $4f$  states treated as localized core states, which yield a work function of 4.0 eV. This value is close to the value for  $\gamma$ -Ce and is much higher than the experimental value.

The description of the ground state in Ce in its different allotropes as well as in many Ce compounds, has been a long and debated subject.<sup>5-13</sup> If a  $4f$  band picture is appropriate to describe the ground state of  $\alpha$ -Ce we might expect the x-ray photoelectron spectra (XPS) to be explained by the calculated one-electron eigenvalues. However, knocking out a  $4f$  electron with x rays can be a strong perturbation on the system, and the XPS data of  $\alpha$ -Ce has been described by either a many-body ground state<sup>19</sup> or by a final-state effect.<sup>20</sup> On the other hand, adding an electron to the valence band (BIS) would in-

crease the screening of the nuclear charge, which in turn makes the wave functions more extended in space. Complicated final-state effects might therefore become suppressed and the BIS signal could possibly be explained by the unoccupied one-electron eigenvalues. In contrast to the XPS spectra, the BIS data of  $\alpha$ - and  $\gamma$ -Ce are different. The spectra of  $\gamma$ -Ce is dominated by a broad peak centered 4 eV above  $E_F$ . This peak has been ascribed to a  $f^2$ , multiplet split, final state. While the spectra of  $\alpha$ -Ce also has this  $f^2$  peak at 4 eV above  $E_F$ , it also has an additional peak pinned at  $E_F$ . A likely explanation for this extra peak pinned at  $E_F$  in  $\alpha$ -Ce is the presence of delocalized  $4f$  states. To investigate this we have calculated the cross sections of the BIS process in a fully relativistic fashion<sup>16</sup> and multiplied them by the orbitally projected DOS. For simplicity we have weighted the surface, subsurface, and bulk atomic contributions to the DOS equally in the calculation. By trying different weightings we have found that the calculated spectra is fairly insensitive to which weighting is used, justifying our simple approach. The lifetime and spectrometer broadening was taken into account by folding the theoretical spectra with a Lorentzian with a full width at half maximum (FWHM) described by  $\Delta = 0.04 (E - E_F)^2$  (in eV) and a Gaussian with a FWHM of 0.7 eV, respectively. The lifetime broadening is not well known either theoretically or experimentally. We have chosen what we think are reasonable values based on other  $f$ -electron calculations we have done. The spectrometer broadening is that appropriate to the reported experimental data. The BIS result is shown in Fig. 5. Notice that the BIS signal of  $\alpha$ -Ce is dominated by a 1-eV broad peak situated just above  $E_F$ . This is in good agreement with experimental data in that energy range<sup>21</sup> with both the width and the position properly described by our calculations. Obviously we cannot from our one-electron approximation account for the localized, multiplet-split,  $f^2$  final state at 4 eV. The present result suggests that there are two different final-state channels for the BIS process in  $\alpha$ -Ce, namely, a delocalized  $4f$  final state (the peak pinned at  $E_F$ ) and a localized  $f^2$  final state (the peak at 4 eV above

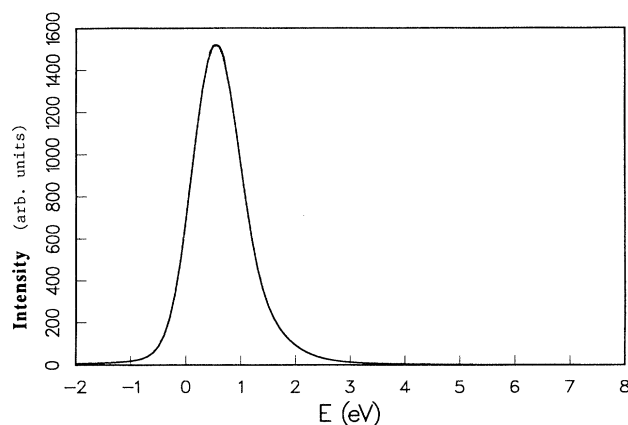


FIG. 5. Calculated BIS intensity of  $\alpha$ -Ce (arbitrary units). Energies are in electron volt and  $E_F$  is at zero.

$E_F$ ). A similar calculation for the  $\gamma$  phase would give a similar one-electron peak at  $E_F$ . The absence of such a peak in the BIS data is consistent with the absence of delocalized  $4f$  states in that phase.

#### IV. CONCLUSION

The first high quality *ab initio* calculations of the surface electronic structure of Ce at both the  $\alpha$  and  $\gamma$  volumes have been presented. We have been able to reproduce sensitive experimental data, such as the work function of  $\alpha$ -Ce, by assuming itinerant  $f$  electrons for this phase. When the  $4f$  states are treated as localized, the calculated work function of  $\alpha$ -Ce is an eV higher than the experimental value. Thus it seems that not only the cohesive properties of the bulk (the cohesive energy, the equilibrium volume, and the bulk modulus),<sup>8,9,11</sup> but also surface sensitive properties, such as the work function, are poorly described with localized  $4f$  electrons in  $\alpha$ -Ce. Our results also indicate that the work function of the  $\gamma$  phase will be higher than that of the  $\alpha$  phase. Furthermore, we find that the low energy part of the measured BIS data of  $\alpha$ -Ce is in agreement with our calculation. These two findings suggest that the electronic structure

of  $\alpha$ -Ce is best described as a delocalized  $4f$  electron system. We have also shown that the direct  $4f$ - $4f$  hopping channel is slightly dominant in the determination of the  $4f$  bandwidth. However, hybridization effects are almost as important, and it has earlier been shown that the interplay between these two effects is strongly dependent on the  $k$  point.<sup>22</sup> In the light actinide metals (Pa, U, Np, and Pu) other calculations<sup>23</sup> have also shown that the direct  $5f$ - $5f$  hopping is the most important, since an estimate of the unhybridized  $5f$  bandwidths is very similar to the calculated hybridized bandwidths. We also find that the surface states of both  $\alpha$ - and  $\gamma$ -Ce are remarkably similar, and therefore we predict that the surface of  $\alpha$ -Ce should undergo a magnetic instability, similar to what was found in bulk  $\gamma$ -Ce.<sup>8</sup>

#### ACKNOWLEDGMENTS

Valuable discussions with B. Johansson, N. Mårtensson, and A. Nilsson are acknowledged. Support from the Nuclear Materials Technology Division at Los Alamos is appreciated. The research at West Virginia University has been supported by NFS Grant No. DMR88-07523.

- 
- <sup>1</sup>For an overview, see D. C. Koskenmaki and K. A. Gschneidner, in *Handbook on the Physics and Chemistry of Rare Earths*, edited by K. A. Gschneidner, Jr. and L. Eyring (North-Holland, Amsterdam, 1978), p. 337.
- <sup>2</sup>F. M. Ellinger and W. H. Zachariasen, *Phys. Rev. Lett.* **32**, 773 (1974); W. H. Zachariasen and F. M. Ellinger, *Acta Crystallogr.* **A33**, 155 (1977).
- <sup>3</sup>J. Staun Olsen, L. Gerward, U. Benedict, and J-P. Itie, *Physica* **133B**, 129 (1985).
- <sup>4</sup>J. Wittig, *Phys. Rev. Lett.* **21**, 1250 (1968).
- <sup>5</sup>W. H. Zachariasen, quoted by A. K. Lawson and T. Y. Tang, *Phys. Rev.* **76**, 301 (1949); L. Pauling, quoted by A. F. Schuck and J. H. Sturdivant, *J. Chem. Phys.* **18**, 145 (1950).
- <sup>6</sup>B. Johansson, *Philos. Mag.* **30**, 469 (1974).
- <sup>7</sup>D. R. Gustafson, J. D. McNutt, and L. O. Roellig, *Phys. Rev.* **183**, 435 (1969); U. Kornstädt, R. Lässer, and B. Lengeler, *Phys. Rev. B* **21**, 1898 (1980).
- <sup>8</sup>D. Glötzel, *J. Phys. F* **8**, L163 (1978).
- <sup>9</sup>W. E. Picket, A. J. Freeman, and D. D. Koelling, *Physica* **120B**, 341 (1980); B. I. Min, H. J. F. Jansen, T. Oguchi, and A. J. Freeman, *Phys. Rev. B* **34**, 369 (1986).
- <sup>10</sup>M. S. S. Brooks, *Physica* **130B**, 6 (1985).
- <sup>11</sup>O. Eriksson, M. S. S. Brooks, and B. Johansson, *Phys. Rev. B* **41**, 7311 (1990).
- <sup>12</sup>J. W. Allen and R. Martin, *Phys. Rev. Lett.* **49**, 1106 (1982); M. Lavagna, C. Lacroix, and M. Cyrot, *Phys. Lett.* **90A**, 710 (1982); *J. Phys. F* **13**, 1007 (1985).
- <sup>13</sup>See articles, in *Handbook on the Physics and Chemistry of Rare Earths* (Ref. 1).
- <sup>14</sup>H. Krakauer and B. R. Cooper, *Phys. Rev. B* **16**, 605 (1977); C. Q. Ma, M. V. Ramana, B. R. Cooper, and H. Krakauer, *ibid.* **34**, 3854 (1986); G. W. Fernando, B. R. Cooper, M. V. Ramana, H. Krakauer, and C. Q. Ma, *Phys. Rev. Lett.* **56**, 2299 (1986).
- <sup>15</sup>S. H. Vosko, L. Wilk, and N. Nusair, *Can. J. Phys.* **58**, 1200 (1980).
- <sup>16</sup>P. Marksteiner, P. Weinberger, R. C. Albers, A. M. Boring, and G. Schadler, *Phys. Rev. B* **34**, 6730 (1986).
- <sup>17</sup>Y. G. Hao, O. Eriksson, G. W. Fernando, and B. R. Cooper (unpublished).
- <sup>18</sup>D. E. Eastman, *Phys. Rev. B* **2**, 2 (1970).
- <sup>19</sup>M. Schlüter and C. M. Varma, in *Valence Instabilities*, edited by P. Wachter and M. Boppart (North-Holland, Amsterdam, 1982), p. 259; A. J. Fedro and S. K. Sinha, *ibid.*, p. 371.
- <sup>20</sup>O. Gunnarson and K. Schönhammer, *Phys. Rev. Lett.* **50**, 604 (1983); J. C. Fuggle, M. Campagna, and Z. Zolnierock, *ibid.* **45**, 1597 (1980); S. Höfner and P. Steiner, in *Valence Instabilities* (Ref. 19), p. 263; S. H. Liu and K.-M. Mo, *Phys. Rev. B* **28**, 4220 (1983); M. R. Norman, D. D. Koelling, A. J. Freeman, H. J. F. Jansen, B. I. Min, T. Oguchi, and L. Ye, *Phys. Rev. Lett.* **53**, 1673 (1984).
- <sup>21</sup>E. Wuilloud, H. R. Moser, W.-D. Schneider, and Y. Baer, *Phys. Rev. B* **28**, 7359 (1983).
- <sup>22</sup>A. M. Boring, R. A. Albers, O. Eriksson, and D. D. Koelling (unpublished).
- <sup>23</sup>M. S. S. Brooks, H. L. Skriver and B. Johansson, in *Handbook on the Physics and Chemistry of the Actinides*, edited by A. J. Freeman and G. H. Lander (North-Holland, Amsterdam, 1984), Vol. 1, p. 153.